


Article

Compact Laser Collimation System for Simultaneous Measurement of Five-Degree-of-Freedom Motion Errors

Chuang Sun ^{1,2} , Sheng Cai ^{1,*}, Yusheng Liu ¹ and Yanfeng Qiao ¹

¹ Changchun Institute of Optics, Fine Mechanics and Physics, Chinese Academy of Sciences, Changchun 130033, China; sunchuang16@mails.ucas.ac.cn (C.S.); liuys@ciomp.ac.cn (Y.L.); qiaoyf@ciomp.ac.cn (Y.Q.)

² College of Materials Science and Opto-Electronic Technology, University of Chinese Academy of Sciences, Beijing 100049, China

* Correspondence: caisheng@ciomp.ac.cn; Tel.: +86-0431-8617-6180

Received: 3 July 2020; Accepted: 19 July 2020; Published: 23 July 2020



Abstract: A compact laser collimation system is presented for the simultaneous measurement of five-degree-of-freedom motion errors. The optical configuration of the proposed system is designed, and the principle of the measurement of five-degree-of-freedom errors is described in detail. The resolution of the roll and the horizontal straightness is doubled compared with other laser collimation methods. A common optical path compensation method is provided to detect light drift in real time and compensate for straightness and angle errors. An experimental setup is constructed, and a series of experiments are performed to verify the feasibility and stability of the system. Compared with commercial instruments, the pitch and yaw residuals are $\pm 2.5''$ and $\pm 3.5''$ without correction, and the residuals are $\pm 1.9''$ and $\pm 2.8''$ after correction, respectively. The comparison deviations of the horizontal straightness and vertical straightness changed from $\pm 4.8 \mu\text{m}$ to $\pm 2.8 \mu\text{m}$ and $\pm 5.9 \mu\text{m}$ to $\pm 3.6 \mu\text{m}$, respectively. The comparison deviation of the roll is $\pm 4.3''$. The experimental results show that the data of the five-degree-of-freedom measurement system obtained are largely the same as the measurement data of commercial instruments. The common optical path compensation can effectively improve the measurement accuracy of the system.

Keywords: 5DOF motion errors; laser collimation; common optical path

1. Introduction

Any object has a 6-degree-of-freedom motion error in space, that is, movement in three axes (positioning, vertical, and horizontal straightness errors) and rotation around three axes (pitch, yaw, and roll). With the rapid development of the manufacturing industry, single-dimensional measuring instruments can no longer meet these measurement needs. A fast, high-precision, and multiple-degree-of-freedom measurement system is urgently needed. The multiple-degree-of-freedom error measurement method can be used not only for the detection of measuring equipment such as CNC machine tools, machining centers, and coordinate measuring machines in the mechanical industry [1–3] but also for the accurate positioning of precise components and relative attitude measurement [4–6].

At present, multiple-degree-of-freedom methods are mainly divided into three types according to the measurement principle: laser interferometry, laser grating diffraction, and laser collimation. Z. Zhang designed a six-degree-of-freedom measurement system by using six improved laser interferometers, which can simultaneously measure a wide range of motion errors. [7]. E. Zhang proposed a laser heterodyne interferometer based on the Faraday effect, which can guarantee the correct interference regardless of the translation or rotation of the measured object [8]. J. Qi proposed a laser heterodyne interferometer based on an acousto-optic modulator for measuring displacement and

roll angle simultaneously. An assembly square pyramidal mirror and a folding mirror are specifically arranged to create a multiple-reflection cavity to increase the roll measurement resolution [9]. B. Chen et al. proposed a laser homodyne straightness interferometer that simultaneously measures six-degree-of-freedom motion errors. The multiple degrees of freedom are measured by the spacing changes and counting of interference fringes [10,11]. This type of measurement method fully utilizes the high-precision characteristics of laser interferometry, but the system is complex and costly.

The laser grating method is based on the principle of grating spectroscopy, which can realize multiple-degree-of-freedom measurements by obtaining different information carried by each beam of separated light. C. Lee et al. proposed a six-degree-of-freedom measurement method by using a single unit of an optical encoder and discussed estimates of the uncertainties in terms of error sources [12,13]. J. Lee proposed a heterodyne grating interferometer for measuring two-dimensional straightness based on a quasi-common optical path (QCOP) [14]. On this basis, H. L. Hsieh proposed a new heterodyne laser interferometer with a six-degree-of-freedom measurement. This technique combined the advantages of heterodyne, Michelson, and grating shear interferometries [15]. Y. Yin proposed a novel structured automatic collimator that can simultaneously measure three-dimensional angles by utilizing Moiré fringes formed by two gratings [16]. However, the angle and position are not linear and the measurement accuracy also changes with the angle in this type of method.

The laser collimation method utilizes the linear propagation characteristics of collimated light, and multiple detectors can be used to detect the position of each beam to achieve multiple-degree-of-freedom measurements. For example, K. C. Fan constructed a three-collimated light six-degree-of-freedom measurement system by using three sets of laser Doppler length gauges. The system has high requirements for the parallelism of the three beams, and adjustment is difficult [17]. W. Wang developed an integrated geometric error optical measurement system for a three-axis miniaturized machine tool and used a homogeneous transformation matrix to calculate the geometric error of six degrees of freedom [18]. In addition, some researchers have used spectroscopic devices to reduce the number of light sources and pyramid prisms [19,20] or special prisms [21–23] as cooperative targets. Q. Feng described a mechanism for improving the measurement resolution of measuring straightness and angular errors [24]. Y. Zhao established a unified measurement model by using the ray-tracing method, to compensate for the measurement errors introduced by the error crosstalk, element fabrication error, laser beam drift, and nonparallelism of two measurement beams [25]. J. Li et al. proposed using a single-mode and fiber-coupled laser as the light source to improve the spatial stability and energy distribution of the measured laser beam [26,27]. This type of measurement method has a simple structure, few optical devices, and low cost.

This paper provides a compact five-degree-of-freedom simultaneous measurement system based on the laser collimation method. Four industrial cameras are used to detect the position of each collimated light spot, to solve all five-degree-of-freedom changes of the measured object. The optical path structure of the measurement system is provided in Section 2, and the measurement methods of straightness and angle error are introduced in detail. We use optical components to make each beam pass through two corner cube retroreflectors, which magnify the lateral movement and roll of the retroreflector twice. This method improves the measurement resolution of roll and horizontal straightness compared to other laser collimation measurement methods. Moreover, a common optical path compensation method is proposed to eliminate the influence of laser beam drift. Finally, an experimental setup is constructed and a series of experiments are performed to verify the feasibility and stability of the system in Section 3.

2. Configuration

Figure 1 shows a schematic diagram of the five-degree-of-freedom measurement system, which consists of a fixed unit and a moving unit. The output beam from a stabilized single-frequency He-Ne laser is a linearly polarized light in the vertical direction. The light is transformed into a circularly polarized light by a quarter wave plate (QWP1), the fast axis of which is set at 45° with the

polarization direction of incident beam. Then, the circularly polarized light is divided into two beams, p-polarized light and s-polarized light, by a polarization beam splitter (PBS1).

The s-polarized light is divided into two beams by the beam splitter (BS1). The reflected light is reflected by mirror (M1) after passing through HWP, PBS3, and QWP2. The reflected light is transformed into s-polarized light through QWP2 twice, and reflected by PBS3. Finally, after passing through L1, the beam is received by complementary metal oxide semiconductor (CMOS3) for measuring pitch and yaw. Section 2.1 is the measuring principle of pitch and yaw.

After passing through RR1, the p-polarized light transmitted by PBS1 is transmitted by BS2, and finally received by CMOS5 camera for measuring straightness error. Section 2.2 is the measuring principle of the straightness error.

The p-polarized light transmitted by PBS1 is reflected by RR1, BS2, M2, and RR2 in turn, and the light is finally received by the CMOS1 camera after passing through PBS2. Compared with the p-polarized light transmitted by PBS1, the s-polarized light transmitted by BS1 is reflected by PBS2 through the opposite path and finally received by CMOS2 camera. The change of the two beams is used to measure the roll. Section 2.3 is the measuring principle of roll.

The s-polarized light transmitted by BS1 is reflected by PBS2, RR2, and M2 in turn, then transmitted through BS2 and L2. Finally, the beam is received by CMOS4 for measuring beam drift. Section 2.4 is the measuring principle of beam drift.

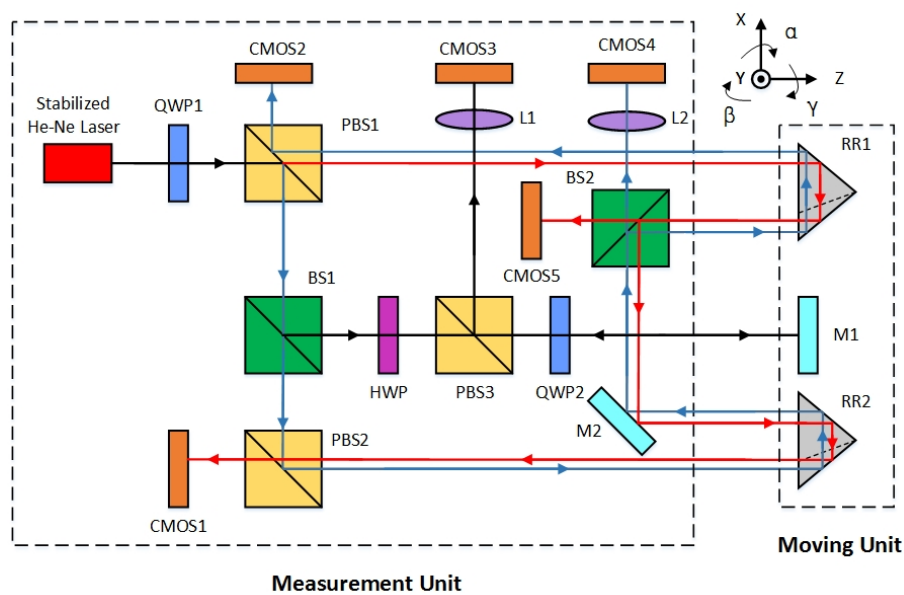


Figure 1. Schematic of the system measuring 5DOF motion errors.

2.1. Pitch and Yaw Measurement

As shown in Figure 2, the plane mirror (M1) is used as a sensitive element in the moving unit to measure pitch and yaw. The reflected s-polarized light by BS1 is converted into p-polarized light by the half wave plate (HWP) and is totally transmitted through the polarization beam splitter (PBS3). The transmitted light is reflected by the plane mirror (M1) and passes through the quarter wave plate (QWP2) twice to be transformed into s-polarized light. The light reflected by PBS3 is finally collected by lens L1 and focused on the image plane, where the CMOS3 camera is placed.

When the moving unit undergoes pitch and yaw movement, the position of the spot changes on the CMOS3 camera. The pitch and yaw are expressed as

$$\alpha = \frac{\Delta Y_{CMOS3}}{2f_1},$$

$$\beta = \frac{\Delta X_{CMOS3}}{2f_1},$$
(1)

where ΔX_{CMOS3} and ΔY_{CMOS3} are the displacements on the CMOS3 camera in the x and y directions, respectively; and f_1 denotes the focal length of L1.

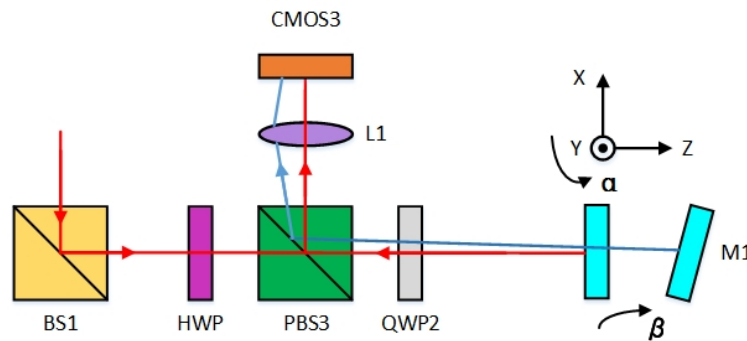


Figure 2. Measurement principle of pitch and yaw.

2.2. Straightness Error Measurement

A schematic diagram of the straightness error measurement based on laser collimation is shown in Figure 3. The light transmitted by PBS1 passes through a corner cube retroreflector (RR1), and the outgoing beam is parallel to the incident beam. The beam is finally received by the CMOS5 camera after passing through BS2.

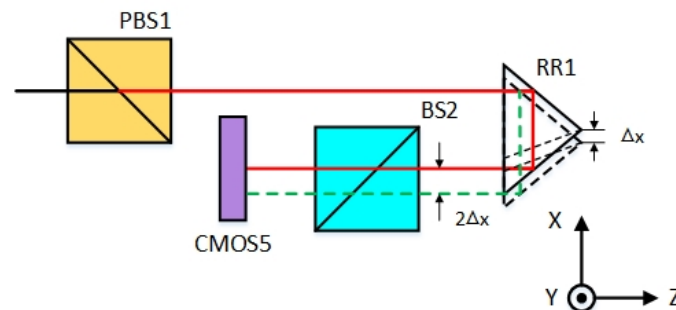


Figure 3. Measurement principle of straightness error.

When the moving unit exhibits straightness errors in the x and y directions, respectively, the position of the spot on the CMOS5 camera changes correspondingly. According to the characteristics of the RRs, when there is a straightness error, the displacement of the spot is doubled, which can be expressed as

$$\Delta x = \frac{\Delta X_{CMOS5}}{2},$$

$$\Delta y = \frac{\Delta Y_{CMOS5}}{2},$$
(2)

where Δx and Δy represent the straightness errors of the moving unit in the x and y directions, respectively; and ΔX_{CMOS5} and ΔY_{CMOS5} denote the displacement of the output laser beam spotted on the CMOS5 cameras.

The horizontal straightness error can also be measured by other beams in Figure 4. The transmitted p-polarized light from PBS1 is reflected by RR1, BS2, M2, and RR2, and received by the CMOS1 camera

after passing through PBS2. The reflective surfaces of BS2 and M2 are placed at 45° with the vertical plane, causing the incident beam to be parallel to the direction of the outgoing beam. In addition, the light reflected by PBS2 travels in the opposite direction, which can also be used for the horizontal straightness error measurement.

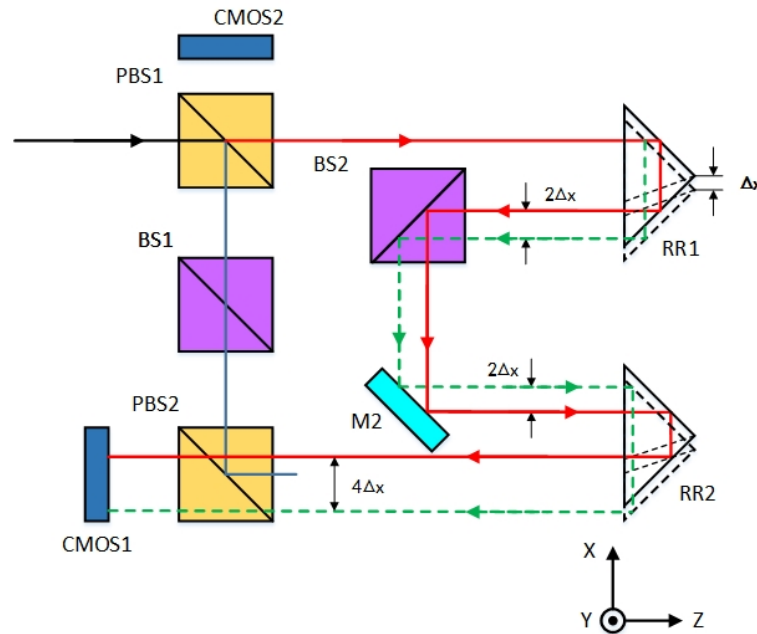


Figure 4. Measurement principle of horizontal straightness error.

Each beam passes through the RR twice compared to Figure 3. When there is a horizontal straightness error Δx , the displacement of the spot is four times, which can be expressed as

$$\Delta x = \frac{\Delta X_{CMOS1}}{4} = \frac{\Delta X_{CMOS2}}{4}, \tag{3}$$

where ΔX_{CMOS1} and ΔX_{CMOS2} denote the displacement of output laser beams in the x direction, which are spotted on the CMOS cameras.

According to Equations (2) and (3), the horizontal straightness can be expressed as

$$\Delta x = \frac{3\Delta X_{CMOS1} + 3\Delta X_{CMOS2} + 4\Delta X_{CMOS5}}{12}. \tag{4}$$

2.3. Roll Measurement

The roll measurement method is based on double parallel beam measurement, using two RRs as sensitive elements. In Figure 5, O1 and O2 indicate the centers of the incident surfaces of RR1 and RR2, respectively. A is the incident point of the measuring beam passing through PBS1, and B is the exit point on RR1. C is the incident point of the measuring beam on RR2, after being reflected by M2 and M3. D is the exit point on RR2, which is finally received by the CMOS1 camera. When there is no roll, the positions of B and C are the same in the y direction. Similarly, the reflected light from PBS2 is incident on RR2, which is finally received by the CMOS2 camera. E and F are the incident and exit points, respectively.

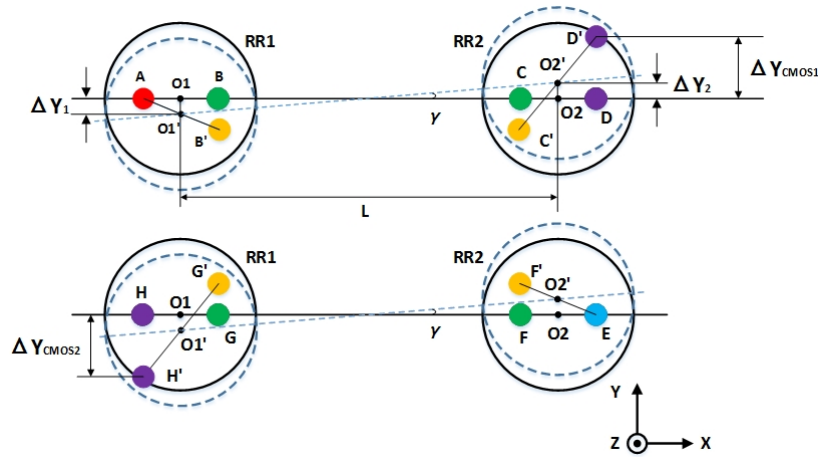


Figure 5. Measurement principle of roll.

When the moving unit produces roll, the position of beam spots will change on RR1 and RR2 except for incident point A. The distance between the center points of the incident surfaces of the two RRs will not change. According to the triangle sine theorem, we can obtain

$$\sin \gamma = \frac{\Delta Y_2 - \Delta Y_1}{L} = \frac{\Delta Y_{CMOS1}}{2L}, \tag{5}$$

where L is the distance between the center points of the incident surfaces of the two RRs; ΔY_2 and ΔY_1 are the position changes of $O1$ and $O2$ in the y direction; and ΔY_{CMOS1} denotes the displacement of output laser beams in the y direction, which is spotted on the CMOS1 cameras.

Similarly, according to another opposite light path, the beam is received by the CMOS2 camera, and we can obtain

$$\sin \gamma = \frac{\Delta Y_2 - \Delta Y_1}{L} = \frac{\Delta Y_{CMOS2}}{2L}, \tag{6}$$

where ΔY_{CMOS2} denotes the displacement of output laser beams in the y direction, which is spotted on the CMOS2 cameras.

Considering that γ is a small angle, the roll can be expressed as

$$\gamma = \frac{\Delta Y_{CMOS2} - \Delta Y_{CMOS1}}{4L}. \tag{7}$$

In other similar methods, a measuring beam passes through an RR only once. However, in the provided system, each beam passes through the RRs twice, which can improve the measurement resolution of roll and horizontal straightness. It is specifically expressed by '4' in Formulas (3) and (6).

2.4. Measurement and Correction of the Laser Beam Drift

The drift of the He-Ne laser beam is mainly affected by temperature, environmental vibration, air disturbance, and the structure of the laser itself. The principle of common light path compensation is shown in Figure 6, which can measure the angular drift of the laser beam in real time.

The incident s-polarized light is reflected by PBS2, RR2, and M2 in turn, and finally received by the CMOS4 camera. The spot displacement on the CMOS4 camera can record the beam drift in real time. The beam angular drift can be expressed as

$$\begin{aligned} \Delta\alpha &= \frac{\Delta Y_{CMOS4}}{f_2}, \\ \Delta\beta &= \frac{\Delta X_{CMOS4}}{f_2}, \end{aligned} \tag{8}$$

where $\Delta\alpha$ and $\Delta\beta$ represent the beam angular drift in the y and x directions; ΔY_{CMOS4} and ΔX_{CMOS4} represent the position of the spot on CMOS4 camera in the x and y directions, respectively; and f_2 is the focal length of L2.

Therefore, Equation (1) of the pitch and yaw can be modified as

$$\begin{aligned} \alpha &= \frac{\Delta Y_{CMOS3}}{2f_1} \pm \Delta\alpha, \\ \beta &= \frac{\Delta X_{CMOS3}}{2f_1} \pm \Delta\beta. \end{aligned} \tag{9}$$

Similarly, the straightness error measurement can be modified as

$$\begin{aligned} \Delta x &= \frac{\Delta X_{CMOS1}}{4} \pm l_1 \Delta\beta \\ &= \frac{\Delta X_{CMOS2}}{4} \pm l_1 \Delta\beta, \\ \Delta y &= \frac{\Delta Y_{CMOS5}}{2} \pm l_2 \Delta\alpha, \end{aligned} \tag{10}$$

where l_1 and l_2 are the distances of light transmitted from the light source to CMOS1, CMOS2, and CMOS5, respectively;

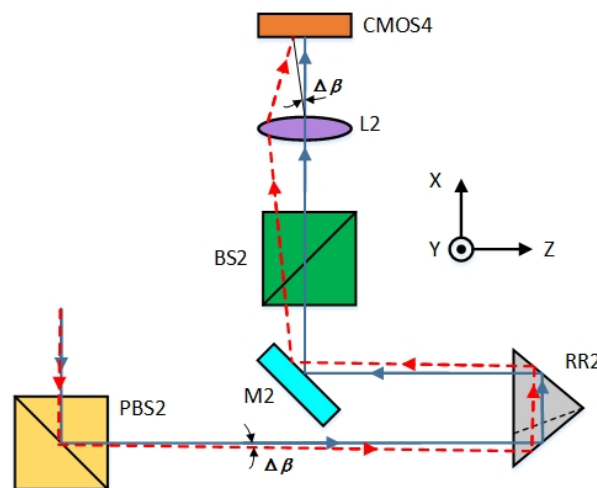


Figure 6. Measurement principle of the angular drift.

3. Experiments and Results

To verify the reliability and effectiveness of the performed method, an experimental setup based on the schematic diagram in Figure 1 was assembled and is shown in Figure 7. The light source is a stable He-Ne laser (HRS015B, Thorlabs, America) with a center wavelength of 632.991 nm, which can achieve frequency stability or intensity stability. The detector used to measure the straightness and roll employs a CMOS sensor (MV-CA050-20GC, HIKROBOT, China) with a resolution of 2592×2048 px and a pixel size of $4.8 \times 4.8 \mu\text{m}$. The focal length of L1 and L2 is 100 mm. The distance between the RRs is 125 mm. The distance between the light source and the moving unit is 500 mm. The distance and focal length do not affect the measurement accuracy, only the measurement resolution. A series of experiments were carried out under laboratory conditions.

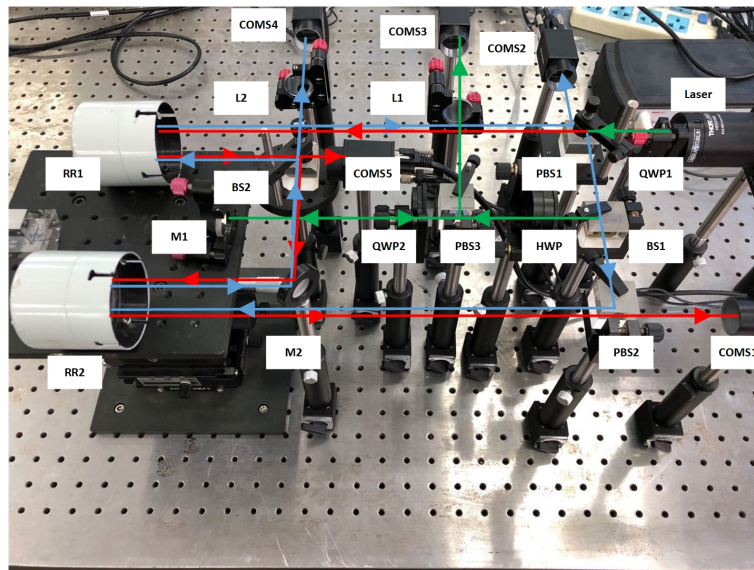


Figure 7. Experimental setup for the five-degree-of-freedom motion error measurement.

3.1. Calibration Experiments

According to the measurement principle described above, in theory, the straightness error and the angle error have a linear relationship with the measured value of the detector. Therefore, the system measurement error can be obtained through calibration experiments.

Figure 8 shows a diagram of the device location for the calibration experiment. A cube prism with five plane mirrors is placed on a six-dimensional moving platform. An interferometric laser encoder (RLE, Britain, accuracy of ± 1 ppm), an industrial theodolite (Leica TM5100A, Switzerland, accuracy of ± 0.5 arcsec), and a standard autocollimator (Taylor Hobson DA400, Britain, accuracy of ± 0.2 arcsec) are used to calibrate various system errors.

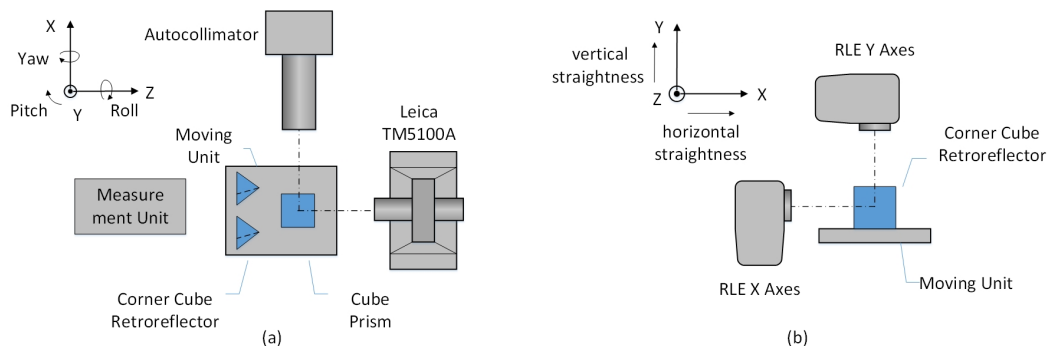


Figure 8. Calibration experiments. (a) Setup for the angle calibration. (b) Setup for the straightness calibration.

As shown in Figure 9, the calibration results are linearly good. In the range of $\pm 360''$, the linear-fit determination coefficient of the pitch and the yaw of the provided system are 1.0000 compared with the Leica TM5100A, the standard deviation of the pitch and the yaw are $0.58''$ and $0.83''$, and the range of fluctuation is from $-1''$ to $1.4''$ and $-1.2''$ to $1.2''$, respectively. In the range of $\pm 360''$, the linear-fit determination coefficient between the roll of the provided system and the autocollimator is 0.9999, the standard deviation is $2.31''$, and the range of fluctuation is from $-5.0''$ to $2.8''$. In the range of $\pm 100 \mu\text{m}$, the linear-fit determination coefficient of horizontal and vertical straightness of the provided system are 0.9996 and 0.9995 compared with RLE, the standard deviations are $1.33 \mu\text{m}$ and $1.4 \mu\text{m}$, and the ranges of fluctuation are from $-1.6 \mu\text{m}$ to $2.8 \mu\text{m}$ and $-1.9 \mu\text{m}$ to $3.1 \mu\text{m}$, respectively.

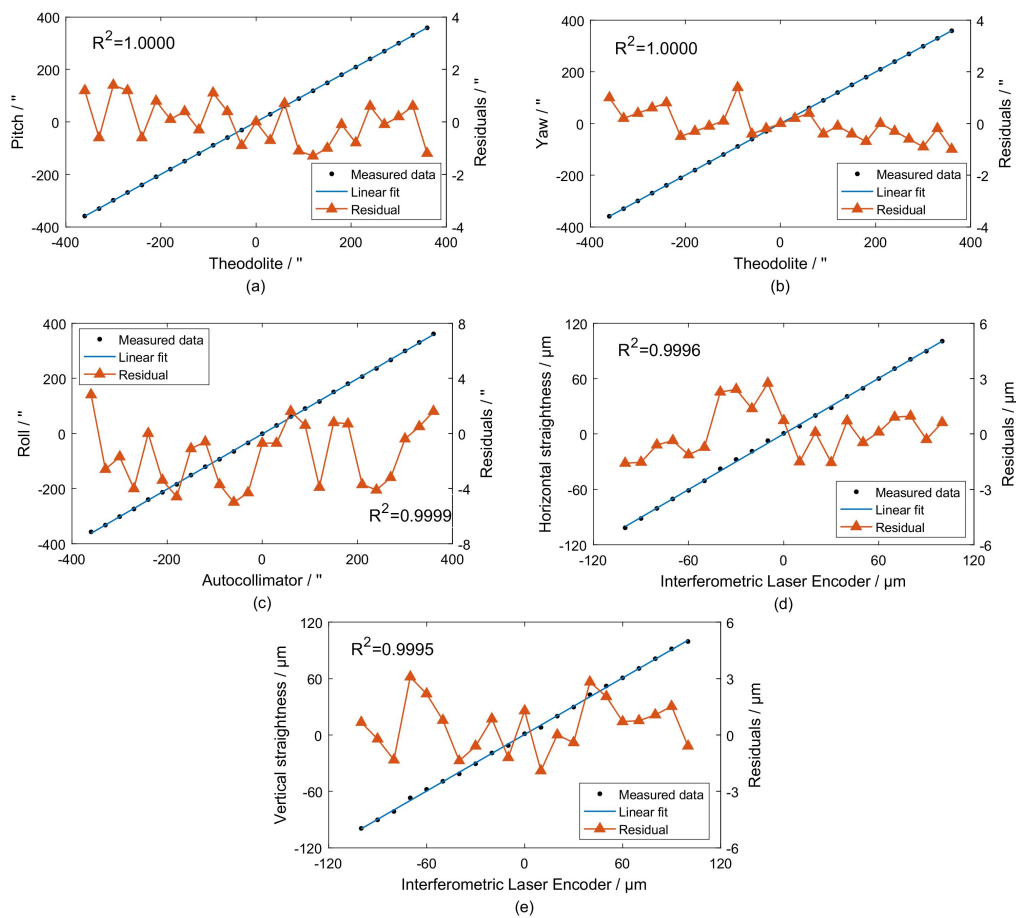


Figure 9. Calibration experiments. (a) Pitch. (b) Yaw. (c) Roll. (d) Horizontal straightness. (e) Vertical straightness.

3.2. Stability Experiments

The stability of the system was tested under laboratory conditions. The range of ambient temperature during the measurement was ± 0.5 °C. The experiment lasted 30 min, and data were collected every 10 s. The measurement results were automatically recorded by the software. The experimental results are shown in Figure 10. The standard deviations of the yaw, pitch, and roll are 0.11 arcsec, 0.11 arcsec, and 0.18 arcsec, respectively. The standard deviations of the horizontal straightness and vertical straightness are 0.38 μm and 0.24 μm , respectively. The above data prove that the proposed system exhibits good stability.

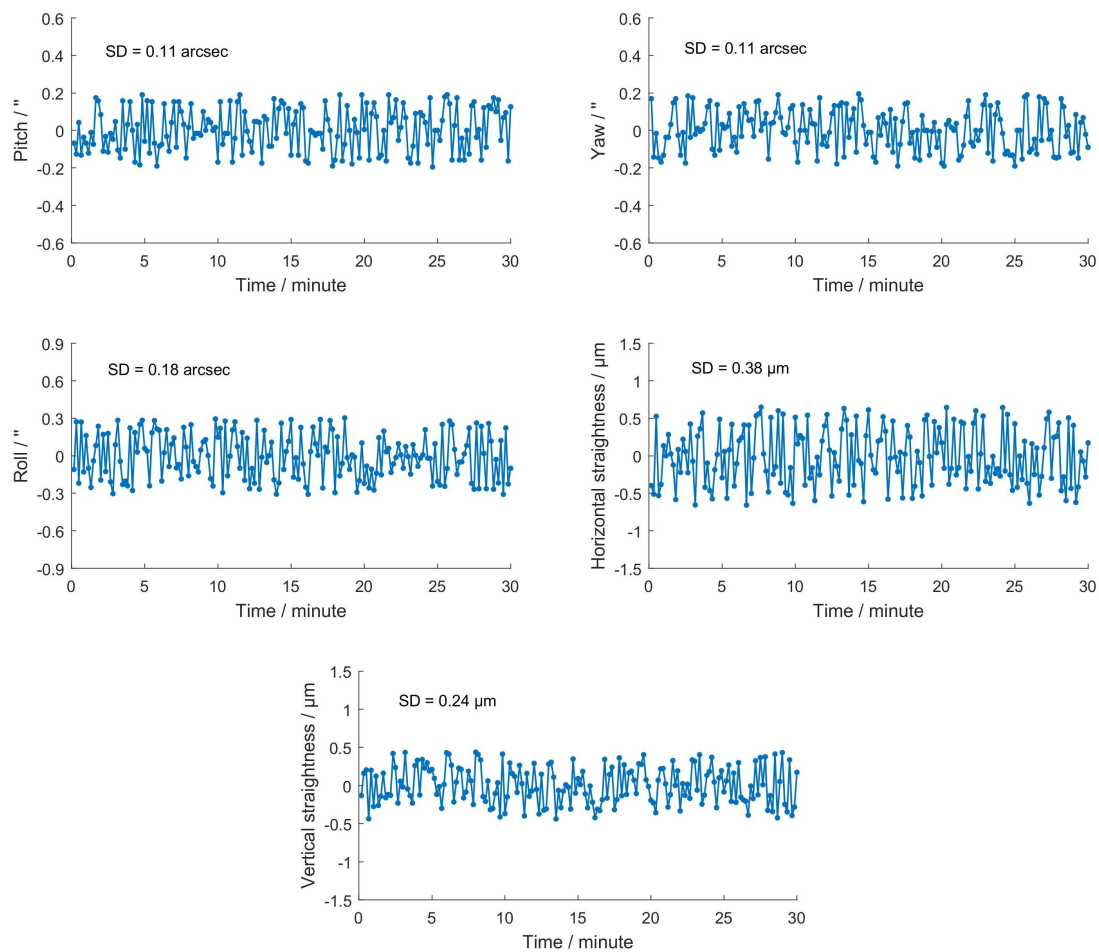


Figure 10. Results of the stability experiments.

3.3. Comparison and Compensation Experiments

The proposed system is compared with commercial instruments for testing. The straightness measurement is compared with the interferometric laser encoder (Renishaw RLE, accuracy of ± 1 ppm). The pitch and yaw were compared with an industrial theodolite (Leica TM5100A, accuracy of ± 0.5 arcsec). The roll was compared with a photoelectric autocollimator (Taylor Hobson DA400, accuracy of ± 0.2 arcsec). The effect of angular drift on the system was analyzed.

The comparison experiments are shown in Figure 11. When the moving stage is 500 mm-away from the light source, the comparison deviations of pitch and yaw are $\pm 2.5''$ and $\pm 3.5''$ without correction, respectively. After the beam drift correction, the comparison deviations of the pitch and the yaw are $\pm 1.9''$ and $\pm 2.8''$, respectively. The comparison deviations of the horizontal straightness and vertical straightness changed from $\pm 4.8 \mu\text{m}$ to $\pm 2.8 \mu\text{m}$ and $\pm 5.9 \mu\text{m}$ to $\pm 3.6 \mu\text{m}$, respectively. The comparison deviation of the roll is $\pm 4.3''$. In addition, we repeated the experiments with the moving stage at a distance of 1 m from the light source to verify the validity of the experimental results. The comparison deviations of the measurements are $\pm 2.0''$ for pitch, $\pm 2.3''$ for yaw, $\pm 4.5''$ for roll, $\pm 2.8 \mu\text{m}$ for horizontal straightness, and $\pm 3.1 \mu\text{m}$ for vertical straightness. From the experimental results, it can be seen that the common light path compensation system can effectively compensate for beam drift.

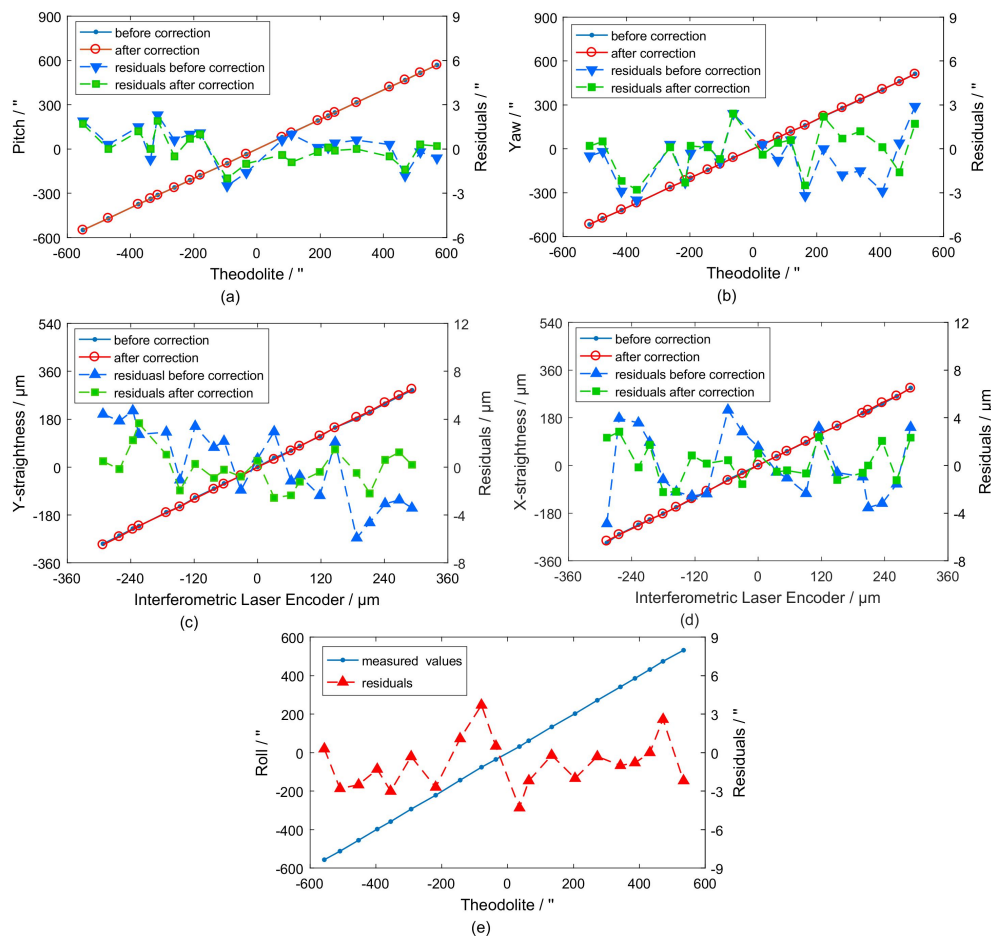


Figure 11. Results of the comparison experiments. (a) Pitch. (b) Yaw. (c) Vertical straightness. (d) Horizontal straightness. (e) Roll.

3.4. Analysis of the Results

Comparing the experimental results in Figure 11 in this paper with those in Figure 10 in Reference [25], the maximum comparison deviation of the horizontal straightness of our system and theirs is within 2.8 μm and 1.5 μm, respectively. The maximum comparison deviation of the vertical straightness is within 3.6 μm and 1.16 μm, respectively. The maximum comparison deviation of the roll is within 4.3'' and 1.01'', respectively. The maximum comparison deviation of the pitch is within 1.9'' and 0.89'', respectively. The maximum comparison deviation of the yaw is within 2.8'' and 0.89'', respectively.

Compared with their system, our system has a larger measurement error. There are three main aspects that affect the measurement accuracy for the provided system, which include beam drift, crosstalk error, and installation and manufacturing errors. Their system analyzed these three errors. According to the above discussion and experiments, the beam drift has been effectively corrected and compensated to improve the measurement accuracy of the system. In theory, crosstalk errors, manufacturing errors, and installation errors can be compensated by ray tracing to establish a mathematical model. Owing to the limitations in length, we will analyze these errors and establish a compensation model in future works.

4. Conclusions

In this paper, a five-degree-of-freedom simultaneous measurement system based on the laser collimation method is proposed. The system uses noncontact cooperative optical measurement, which has the advantages of compact structure, low cost, and high accuracy. The principle of each error

of the system is introduced in detail. In theory, the roll and horizontal straightness of the proposed system of the resolution are higher than those of other measuring systems. The common optical path compensation method is proposed to correct beam drift. Finally, an experimental setup is constructed, and stability experiments, calibration experiments, and comparison compensation experiments are carried out. The experimental results verify the reliability and effectiveness of the proposed system. All these results indicate that the proposed system could be applied in precision measurement and calibration fields.

Author Contributions: Conceptualization, methodology, Y.Q., C.S., and S.C.; validation, C.S. and Y.L.; writing—original draft preparation, writing—review and editing, visualization, C.S.; supervision, project administration, funding acquisition, Y.Q. and S.C. All authors have read and agreed to the published version of the manuscript.

Funding: This work was supported by Youth Innovation Promotion Association, CAS (2019226).

Conflicts of Interest: The authors declare no conflict of interest.

References

1. Ekinci, T.O.; Mayer, J.R.R.; Cloutier, G.M. Investigation of accuracy of aerostatic guideways. *Int. J. Mach. Tools Manuf.* **2009**, *49*, 478–487. [[CrossRef](#)]
2. Huang, Y.; Fan, K.C.; Wei, S.; Liu, S. Low cost, compact 4-DOF measurement system with active compensation of beam angular drift error. *Opt. Express* **2018**, *26*, 17185–17198. [[CrossRef](#)] [[PubMed](#)]
3. Zhang, E.; Chen, B.; Sun, J.; Yan, L.; Zhang, S. Laser heterodyne interferometric system with following interference units for large X-Y- θ planar motion measurement. *Opt. Express* **2017**, *25*, 13684–13690. [[CrossRef](#)] [[PubMed](#)]
4. Yan, H.; Duan, H.Z.; Li, L.T.; Liang, Y.R.; Luo, J.; Yeh, H.C. A dual-heterodyne laser interferometer for simultaneous measurement of linear and angular displacements. *Rev. Sci. Instrum.* **2015**, *86*, 123102. [[CrossRef](#)] [[PubMed](#)]
5. Yang, J.; Wang, D.; Fan, B.; Dong, D.; Zhou, W. Online absolute pose compensation and steering control of industrial robot based on six degrees of freedom laser measurement. *Opt. Eng.* **2017**, *56*, 034111.1–034111.9. [[CrossRef](#)]
6. Guo, Y.; Cheng, H.; Wen, Y.; Feng, Y. Three-degree-of-freedom autocollimator based on a combined target reflector. *Appl. Opt.* **2020**, *59*, 2262–2269. [[CrossRef](#)]
7. Zhang, Z.; Menq, C.H. Laser interferometric system for six-axis motion measurement. *Rev. Sci. Instrum.* **2007**, *78*, 083107. [[CrossRef](#)]
8. Zhang, E.; Hao, Q.; Chen, B.; Yan, L.; Liu, Y. Laser heterodyne interferometer for simultaneous measuring displacement and angle based on the Faraday effect. *Opt. Express* **2014**, *22*, 25587–25598. [[CrossRef](#)]
9. Jingya, Q.; Zhao, W.; Junhui, H.; Jianmin, G. Laser heterodyne interferometer for simultaneous measurement of displacement, and roll-angle based on the acousto-optic modulators. *Proc. SPIE* **2019**, *10678*, 1067806.
10. Chen, B.; Xu, B.; Yan, L.; Zhang, E.; Liu, Y. Laser straightness interferometer system with rotational error compensation and simultaneous measurement of six degrees of freedom error parameters. *Opt. Express* **2015**, *23*, 9052–9073. [[CrossRef](#)]
11. Lou, Y.; Yan, L.; Chen, B.; Zhang, S. Laser homodyne straightness interferometer with simultaneous measurement of six degrees of freedom motion errors for precision linear stage metrology. *Opt. Express* **2017**, *25*, 6805–6821. [[CrossRef](#)]
12. Lee, C.B.; Kim, G.H.; Lee, S.K. Design and construction of a single unit multi-function optical encoder for a six-degree-of-freedom motion error measurement in an ultraprecision linear stage. *Meas. Sci. Technol.* **2011**, *22*, 105901. [[CrossRef](#)]
13. Lee, C.B.; Kim, G.H.; Lee, S.K. Uncertainty investigation of grating interferometry in six degree-of-freedom motion error measurements. *Int. J. Precis. Eng. Manuf.* **2012**, *13*, 1509–1515. [[CrossRef](#)]
14. Lee, J.Y.; Hsieh, H.L.; Lerondel, G.; Deturche, R.; Lu, M.P.; Chen, J.C. Heterodyne grating interferometer based on a quasi-common-optical-path configuration for a two-degrees-of-freedom straightness measurement. *Appl. Opt.* **2011**, *50*, 1272–1279. [[CrossRef](#)] [[PubMed](#)]

15. Hsieh, H.L.; Pan, S.W. Development of a grating-based interferometer for six-degree-of-freedom displacement and angle measurements. *Opt. Express* **2015**, *23*, 9052–9073. [[CrossRef](#)]
16. Yin, Y.; Sheng, C.; Qiao, Y. Design, fabrication, and verification of a three-dimensional autocollimator. *Appl. Opt.* **2016**, *55*, 9986–9991. [[CrossRef](#)] [[PubMed](#)]
17. Fan, K.C.; Chen, M.J.; Huang, W.M. A six-degree-of-freedom measurement system for the motion accuracy of linear stages. *Int. J. Mach. Tools Manuf.* **1998**, *38*, 155–164. [[CrossRef](#)]
18. Wang, W.; Kweon, S.H.; Hwang, C.S.; Kang, N.C.; Kim, Y.S.; Yang, S.H. Development of an optical measuring system for integrated geometric errors of a three-axis miniaturized machine tool. *Int. J. Adv. Manuf. Technol.* **2009**, *43*, 701–709. [[CrossRef](#)]
19. Cui, C.; Feng, Q.; Zhang, B. Compensation for straightness measurement systematic errors in six degree-of-freedom motion error simultaneous measurement system. *Appl. Opt.* **2015**, *54*, 3122–3131. [[CrossRef](#)]
20. Li, J.; Feng, Q.; Bao, C.; Zhao, Y. Method for simultaneous measurement of five DOF motion errors of a rotary axis using a single-mode fiber-coupled laser. *Opt. Express* **2018**, *26*, 2535–2545. [[CrossRef](#)]
21. Huang, P.; Li, Y.; Wei, H.; Ren, L.; Zhao, S. Five-degrees-of-freedom measurement system based on a monolithic prism and phase-sensitive detection technique. *Appl. Opt.* **2013**, *52*, 6607–6615. [[CrossRef](#)] [[PubMed](#)]
22. You, F.; Feng, Q.; Zhang, B. A new five degree-of-freedom measurement method and system. *Proc. SPIE* **2009**, *7156*, 715634.
23. Zhang, T.; Feng, Q.; Cui, C.; Zhang, B. Research on error compensation method for dual-beam measurement of roll angle based on rhombic prism. *Chin. Opt. Lett.* **2014**, *12*, 71201–71204. [[CrossRef](#)]
24. Qibo, F.; Bin, Z.; Cunxing, C.; Cuifang, K.; Yusheng, Z.; Fenglin, Y. Development of a simple system for simultaneously measuring 6DOF geometric motion errors of a linear guide. *Opt. Express* **2013**, *21*, 25805–25819. [[CrossRef](#)]
25. Zhao, Y.; Zhang, B.; Feng, Q. Measurement system and model for simultaneously measuring 6DOF geometric errors. *Opt. Express* **2017**, *25*, 20993–21007. [[CrossRef](#)] [[PubMed](#)]
26. Li, J.; Feng, Q.; Bao, C.; Zhang, B. Method for simultaneously and directly measuring all six-DOF motion errors of a rotary axis. *Chin. Opt. Lett.* **2019**, *17*, 011203.
27. Cui, C.; Feng, Q.; Zhang, B.; Zhao, Y. System for simultaneously measuring 6DOF geometric motion errors using a polarization maintaining fiber-coupled dual-frequency laser. *Optics Express* **2016**, *24*, 6735–6748. [[CrossRef](#)]



© 2020 by the authors. Licensee MDPI, Basel, Switzerland. This article is an open access article distributed under the terms and conditions of the Creative Commons Attribution (CC BY) license (<http://creativecommons.org/licenses/by/4.0/>).